Journal of Magnetic Resonance **145,** 326–333 (2000)
doi:10.1006/jmre.2000.2094, available online at http://www.idealibrary.com on IDEAL®

Separation of the Ortho and Para NMR Signals in Solid Deuterium via DQ Filtering

Pekka Malmi,* Matti Punkkinen,* Eero Ylinen,* and Valeri Shevtsov†

**Wihuri Physical Laboratory, Department of Physics, University of Turku, FIN-20014 Turku, Finland; and †Russia Research Center "Kurchatov Institute," 123182 Moscow, Russia*

E-mail: pekmalmi@utu.fi; vash@orc.ru

Received January 21, 2000; revised March 28, 2000

Double quantum (DQ) filtering is shown to lead to an effective separation of the NMR signals from the para ($I = 1$) and ortho ($I = 2$) molecules in solid deuterium. The separation is achieved by the pulse sequence $90°_{\phi}$–t_{pr}–$90°_{\phi}$–t_{ev}–$90°_{\bar{x}}$–t, where the phase-cycled first two pulses create the DQ coherence. Two components are observed after the third pulse; the para signal shows the maximum at a short time t while the ortho signal reaches the maximum at a longer t. The observed signal can be expressed as $\frac{1}{2}\sum_I [F_I(t_{pr} - t) - F_I(t_{pr} + t)]$, where $F_I(t)$ is a proper fitting function for the free induction signal of the para and ortho molecules (with $I = 1$ or 2, respectively). Numerical fits to experimental data at 4.2 and 2 K show that this method can be used to determine the ratio $F_1(0)/F_2(0)$ and thus, because the initial value $F_I(0)$ is proportional to the respective magnetization before the pulse sequence, the ortho and para concentrations in solid deuterium.

Key Words: **NMR of solid deuterium; double quantum filtering; ortho and para concentrations.**

1. INTRODUCTION

One of the challenges in NMR studies of solid deuterium is the determination of the concentration of ortho and para molecules. An attractive method would be to observe the free induction signal (FID) and separate the corresponding components in it. Unfortunately, this approach meets considerable difficulties in solid deuterium. The ortho molecules with the total nuclear spin $I = 2$, which at low temperatures are mainly in the rotational ground state $J = 0$, are responsible for a rather slowly decaying and only weakly temperature-dependent component in FID. On the other hand, the electric quadrupole–quadrupole (EQQ) interaction between the para-D_2 molecules with the total nuclear spin $I = 1$, which are mainly in the first excited rotational state $J = 1$, leads to a fast-decaying and strongly temperature-dependent component (*1, 2, 3, 6*). The strong variation with temperature originates from the orientational ordering via the EQQ interaction between para molecules. Also the ortho molecules undergo a weak orientational ordering because of the interaction with the oriented para molecules.

According to the Curie law the amplitude A_I of the FID components is proportional to $I(I + 1)$. The ortho molecules have five possible spin states for $I = 2$ and one for $I = 0$, which are all equally populated (except at very low temperatures and high magnetic fields). Since the molecules with $I = 0$ give no NMR signal, only the fraction $\frac{5}{6}$ of the ortho molecules contributes to the ortho component in FID. Hence, the amplitude ratio of the FID components of the para and ortho molecules is given by

$$R = \frac{A_1}{A_2} = \frac{2X}{5(1 - X)}, \qquad [1]$$

where X is the relative para concentration. If solid deuterium is in thermal equilibrium at a relatively high temperature ($\geq$100 K), one-third of the molecules is in the para state so that $X = 0.33$ and $R = 0.2$. After cooling down to liquid helium temperatures the sample starts to approach thermal equilibrium, but extremely slowly. At 4.2 K when $X \approx 0.33$ the para–ortho conversion proceeds at the rate of 0.02% per hour which in R means only a decrease of about 0.4% per day (*7*). Thus R is practically constant if NMR measurements take only few days.

In pulsed NMR of solids, especially at low temperatures, a frequently encountered problem is the information lost under the dead time, or the time the receiver of the spectrometer is shocked by the strong RF pulse. For example, in solid deuterium the EQQ interaction makes the para component of FID decay so fast that the relevant information is lost. Furthermore, there is no universal signal shape which would allow an extrapolation back to the center of the RF pulse. Various methods have been adopted in order to overcome this problem, among which the solid echo is most popular. Unfortunately, the solid echo does not always reflect the magnetizations of the ortho and para molecules in such a simple way as the partial FID amplitudes or the areas of the different spectral components in the corresponding Fourier transform (FT), provided that the latter procedures could be carried out reliably. Anomalous

1090-7807/00 $35.00

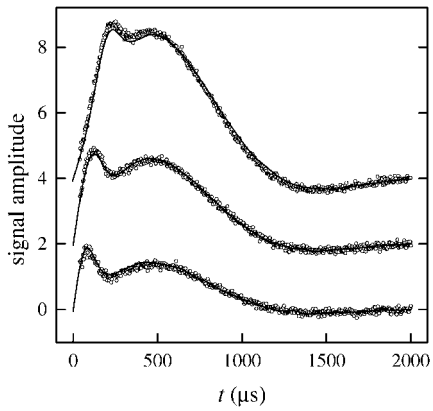

FIG. 1. Comparison of experimental (open circles) and calculated (Eq. [8], solid line) DQ filtered signals at 4.2 K with $t_{pr} = 50$, 100, and 200 μs from bottom to top, respectively. Only one parameter, the proportionality factor A, is determined by least-squares fitting.

behavior of the solid echo in solid D_2 was reported and discussed in Refs. (*3–6*).

The FID method for concentration determination can be utilized in a limited temperature range by using a very short but intensive 90° pulse and by decreasing the dead time. Unfortunately, such improvements lose their advantage at lower temperatures, where the decay rate of the para signal increases. Here we introduce a method based on the creation and detection of the double quantum (DQ) coherence, in which the relevant part of the signal is not affected by the dead time. The pulse sequence consists of three strong RF pulses: 90°_ϕ–t_{pr}–90°_ϕ–t_{ev}–90°_x–t, where ϕ refers to the phase of the pulse. The first two pulses, separated by the preparation time t_{pr}, create the DQ coherence (*8–10*). All of the other coherences are filtered off by a phase cycling. The cycles repeated are $\{x, y, -x, -y\}$ and $\{y, -y\}$ for the first two pulses and the receiver, respectively. In our experiments, carried out at the exact resonance, the evolution time t_{ev} was made quite short to avoid unnecessary decrease of the DQ coherence amplitude. The third pulse transforms this coherence back to an observable form.

In all of our experiments the DQ signal started from zero and developed two maxima (Fig. 1). The most interesting feature is the first narrow peak at a small t, which turned out to reflect the population of the para molecules. The ortho molecules give rise to the other, broader maximum at a larger value of t. The position of the first peak shifts toward larger t with increasing t_{pr}. The maximum itself is more pronounced than the corresponding peak in solid echo, especially after short preparation times, which makes the DQ filtering a very promising tool for the exact determination of the signal ratio R.

2. THEORY

The DQ filtering experiment of spins $I = 1$ after the described three-pulse sequence was already treated in Ref. (*10*) in the case of strong RF pulses. Below the derivation is pursued to a more advanced point, where the general correspondence between the FID and DQ signals is found. The dominant interaction of the nuclear spins is that with the external magnetic field $\mathbf{B}_0$ corresponding to the Hamiltonian $H_z = -\gamma\hbar B_0 \sum I_z$, where γ is the deuteron gyromagnetic ratio and I_z the spin operator. In usual NMR experiments H_z is at least two orders of magnitude larger than the nuclear quadrupole interaction of the para molecules. Therefore it is sufficient to retain only the secular part of the quadrupole interaction,

$$H_Q = \omega_Q(3I_z^2 - I^2)/3, \qquad [2]$$

with

$$\omega_Q = (3\cos^2\theta - 1 + \eta\sin^2\theta\cos 2\varphi)3e^2qQ/8\hbar, \qquad [3]$$

where e^2qQ is the quadrupole coupling constant, η is the asymmetry parameter, and θ and φ are the polar angles of $\mathbf{B}_0$ in the principal axis frame of the quadrupole interaction. It is important to notice that ω_Q varies with the crystal orientation. For each crystal orientation the corresponding NMR spectrum is a doublet with the separation $2\omega_Q$.

In thermal equilibrium, which is assumed to be the initial state of the system, the density operator $(1/Z)\exp(-H_z/kT_L)$ can be written as $\sigma_{eq} = bI_z$, where the constant part is dropped off as unsignificant. The multiplier b equals $\hbar\omega_0/ZkT_L$, where k, Z, T_L, and $\omega_0 = \gamma B_0$ are the Boltzmann constant, the partition function, the sample temperature, and the resonance frequency in angular units, respectively. The time dependence of σ in the frame rotating at the exact resonance frequency ω_0 relative to the laboratory frame is calculated from the equation $d\sigma/dt = (i/\hbar)[\sigma, \tilde{H}]$, where $\tilde{H}$ denotes the Hamiltonian expressed in the rotating frame. During strong RF pulses at exact resonance $\tilde{H}$ equals $-\gamma\hbar B_1 \sum I_x$, where B_1 is the amplitude of the RF magnetic field. Between the pulses and after them $\tilde{H} = H_Q$ as given in Eq. [2]. The magnetic dipolar interaction between the deuterons in a para molecule is about 10 times smaller than H_Q (*3, 6*) and can thus be ignored.

Next we consider the behavior of the para molecules in the rotating frame during the first three-pulse sequence ($\phi = x$). The first 90°_x pulse turns the para magnetization along the y axis, which means that $\sigma_{pr}(0) = bI_y$. During the preparation period the variation of $\sigma_{pr}(t)$ is easier to calculate by using so-called single transition operators $I_\alpha^{(jk)}$, where α is the cartesian component x, y, or z in the rotating frame and the superindices j and k indicate that the transition between the Zeeman states j and k is involved (*8*). The quadrupole Hamiltonian of Eq. [2] produces the time dependence

$$\sigma_{pr}(t) = \sqrt{2}b[(I_y^{(12)} + I_y^{(23)})\cos\omega_Q t + (-I_x^{(12)} + I_x^{(23)})\sin\omega_Q t]. \qquad [4]$$

The second 90°_x pulse transforms the density operator $\sigma_{pr}(t_{pr})$ to

$$\sigma_{ev}(0) = -2b(I_z^{(13)}\cos\,\omega_Q t_{pr} + I_y^{(13)}\sin\,\omega_Q t_{pr}) \qquad [5]$$

where $I_y^{(13)}$ is the desired operator for the DQ coherence. The contribution of $I_z^{(13)}$ is removed by a proper phase cycling. In order to avoid unnecessary decay of the DQ coherence, the third pulse is applied almost immediately after the second one. The 90°_x pulse transforms $-2bI_y^{(13)}$ into a single quantum coherence, which varies during the acquisition period as

$$\sigma_{ac}(t) = \sqrt{2}b[(I_x^{(12)} - I_x^{(23)})\cos\,\omega_Q t + (I_y^{(12)} + I_y^{(23)})\sin\,\omega_Q t]. \qquad [6]$$

The latter term in Eq. [6] produces a signal proportional to $\sin\,\omega_Q t$. Each spectral component, resonating at ω_Q relative to the exact resonance frequency ω_0, yields its own maximum at $t = \pi/2\omega_Q$. According to (*9*) we call the efficiency of the pulse sequence, in creating the DQ coherence among different spectral components and transforming it into observable form, the *DQ transfer function*, which in our case equals $\sin\,\omega_Q t_{pr}\sin\,\omega_Q t$ (cf. Eqs. [5] and [6]). Each spectral component then contributes to the observable signal by an amount

$$dS_{DQ}(t_{pr}, t) = Ag(\omega_Q)\sin\,\omega_Q t_{pr}\sin\,\omega_Q t d\omega_Q. \qquad [7]$$

Here $g(\omega_Q)$ is the normalized absorption curve of the para molecules and the proportionality factor A is determined by the number of para molecules, the receiver amplification, the number of turns in the sample coil, and other experimental factors. When the contribution of all the spins $I = 1$ (para molecules) in the sample is taken into account, the DQ filtered signal becomes

$$S_{DQ}(t_{pr}, t) = A\int_{-\infty}^{\infty} g(\omega_Q)\sin\,\omega_Q t_{pr}\sin\,\omega_Q t d\omega_Q. \qquad [8]$$

If the induction signal of the same sample is observed under exactly identical experimental conditions its intensity will be

$$S_{FID}(t) = A\int_{-\infty}^{\infty} g(\omega_Q)\cos\,\omega_Q t d\omega_Q. \qquad [9]$$

By using Eq. [9] and the well-known trigonometric identity $\sin x\,\sin y = \frac{1}{2}[\cos(x - y) - \cos(x + y)]$, Eq. [8] becomes

$$S_{DQ}(t_{pr}, t) = \tfrac{1}{2}[S_{FID}(t_{pr} - t) - S_{FID}(t_{pr} + t)]. \qquad [10]$$

Thus the DQ filtered signal after the three-pulse sequence can be expressed in terms of the corresponding FID function, but evaluated at shifted times $t_{pr} \pm t$. It can be seen easily from Eq. [10] that $S_{DQ} = 0$ for $t = 0$.

For the present method to be reliable, the RF pulses must fulfill the condition $\gamma B_1 = \omega_1 > \omega_Q$. In the case of polycrystalline solid deuterium this condition means that $\omega_1 > 3e^2qQ/4\hbar$. If ω_1 and ω_Q are of equal magnitude, the signal S_{DQ} will contain many terms. The one corresponding to Eq. [7] is

$$dS_{DQ} = Ag(\omega_Q)(\omega_1/F)^3\sin\,Ft_{p1}\sin\,Ft_{p2}\sin\,Ft_{p3} \times \sin[\omega_Q(t_{pr} + \tfrac{1}{2}t_{p1} + \tfrac{1}{2}t_{p2})] \times \sin[\omega_Q(t + \tfrac{1}{2}t_{p3})]d\omega_Q, \qquad [11]$$

where $F = (\omega_1^2 + \omega_Q^2/4)^{1/2}$. The lengths of the successive pulses are t_{p1}, t_{p2}, and t_{p3}, and the RF field is assumed to have the same amplitude during all these pulses. Although the term in Eq. [11] cannot be used alone instead of Eq. [7], it gives a possibility of evaluating the magnitude of the error when Eq. [10] is used. In addition it shows that the lengths of the RF pulses contribute to the preparation and acquisition times.

Unfortunately, the present derivation is valid only for spins with $I = 1$, when the quadrupole interaction dominates the spectral shape. A similar calculation could also be performed for the ortho molecules with $I = 2$ if H_Q were the dominant factor determining the NMR absorption curve. Then, instead of $\sin\,\omega_Q t_{pr}\sin\,\omega_Q t$ in Eqs. [7] and [8] there would be a more complicated function. Even such derivations cannot be used in the case of ortho molecules in solid deuterium, because the magnetic dipolar interaction between neighboring molecules is known to have an important role in the NMR spectrum. Therefore, when we use Eq. [10] to describe the dependence of S_{DQ} of ortho molecules on the times t_{pr} and t, the only justification is its good agreement with the experimental data.

3. RESULTS AND DISCUSSION

As pointed out above, the derivation of Eq. [10] is strictly speaking valid only for spins $I = 1$. Its validity for spins $I = 2$ was, however, tested empirically in a straightforward way by comparing the curves calculated from Eq. [8] with a series of DQ filtered signals measured with different preparation times t_{pr}. The absorption curve $Ag(\omega_Q)$, used in the numerical integration, was the Fourier transform of the experimental FID measured under the same experimental conditions as the DQ signals. In all DQ experiments listed here the evolution time t_{ev} was 10 μs while the preparation time t_{pr} varied from 25 to 200 μs. As shown in Fig. 1, the calculated curves follow very well the behavior of the experimental DQ signals. We want to emphasize that each calculated curve contains only one parameter, the overall scaling factor, which was equal for both the ortho and the para signals.

A critical examination of Fig. 1 shows, however, that the maximum of the para component for short t is slightly under-

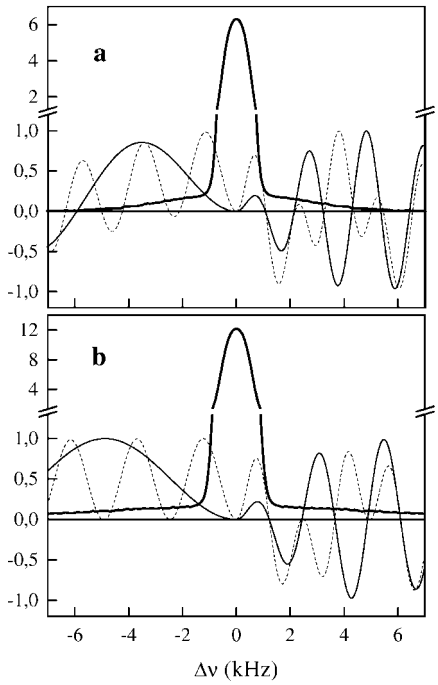

FIG. 2. Solid D_2 absorption curves (thick lines) at 4.2 K (a) and 2 K (b) and examples of the DQ transfer function $\sin \omega_Q t_{pr} \sin \omega_Q t$ with $t_{pr} = 50$ μs (solid lines) and 200 μs (dashed lines). On the positive side t is long (410–466 μs), corresponding to the broad maxima in Fig. 4, while on the negative side t is shorter (52–236 μs), corresponding to the narrow DQ maxima.

estimated. Thus, it is worth noting that the inaccuracy in FID, originating from the dead time, appears in the FT as an oscillating baseline. That happens if the FT is calculated correctly by replacing the unreliable points by zero instead of just shifting the zero time to the first reliable point. In the case of the very fast decaying para signal the amplitude of the baseline oscillation was much higher than the amplitude of the spectrum itself. Understandably, the baseline-corrected spectrum may then contain errors. The most sensitive part of the calculated DQ curve for possible errors in the baseline correction is the narrow maximum at short t which is determined by the broad and weak para spectrum (Fig. 2).

The absorption curves of solid deuterium at 4.2 and 2 K and examples of the DQ transfer function, with the values of t corresponding to the two maxima of the DQ filtered signal, are shown in Fig. 2. Actually the DQ transfer function is symmetric relative to the center of the absorption curve, but for brevity we show the curves for narrow and broad maxima on opposite sides of the center. The transfer function with t corresponding to the narrow maxima of the DQ signals with short t_{pr} (solid curves plotted for negative values of $\Delta\nu$) obviously picks out the broad component of the absorption curve whereas the corresponding function with long t_{pr} (dashed curves on the negative side) is effective also under the intense central peak. This indicates that the separation of the ortho and para signals works better with shorter preparation times. The transfer functions on the positive side, producing the broad maxima of the DQ filtered signal, have a positive half-cycle under the intense narrow peak while the oscillations for larger $\Delta\nu$ values tend to average out the contribution from broad parts of the spectra. Also the separation resulting from this averaging seems to work better with shorter preparation times.

The examples in Fig. 2 suggest that the DQ transfer function becomes more selective with decreasing preparation time. This is demonstrated also in Fig. 1, where decreasing t_{pr} results in a decreasing overlap of the maxima. However, it is not possible to separate the DQ filtered ortho and para signals completely, because both of them start from zero time (cf. Eq. [10]). Thus, a fitting function, consisting of independent ortho and para parts, is required for the determination of the amplitude ratio R. For shorter t_{pr} there is less correlation between the parameters belonging to the different parts of the fitting function. However, the choice of the optimal preparation time is not so straightforward because longer t_{pr} gives better signal-to-noise ratio which compensates, at least partly, for the decreasing separation of the signals. In order to find the optimal conditions we worked out a brief statistical analysis of a series of DQ filtered signals.

The good fit of the calculated and measured curves shown in Fig. 1 suggests that the best fit of Eq. [10] to the DQ filtered signal requires only a small adjustment of the best-fit FID parameters determined from the induction signal measured under the same experimental conditions. This is of great help in searching for a proper fitting function, since good candidates for FID can be found in the literature. We tested different combinations of three analytical functions. The ortho signal requires inevitably a fitting function, which is able to reproduce damped oscillations in FID. The simplest such function, widely used in solid state NMR studies is (*11–13*)

$$f_{gs} = A \exp(-at^2)\sin bt/bt.$$

A second candidate for fitting the ortho signal is obtained by replacing the sine function in f_{gs} with the first-order Bessel function J_1 (*12, 14*),

$$f_{gj} = 2A \exp(-at^2)J_1(bt)/bt.$$

This is supposed to give a better result than f_{gs} if the zero crossings of the induction signal are not equally spaced. Actually, the FIDs show such behavior (cf. Fig. 5a) but the statistical analysis still proved f_{gs} slightly better. For the para signal we adopted a simple gaussian,

$$f_g = A \exp(-at^2),$$

with only two adjustable parameters. The fitting of the oscillating function f_{gs} to the para signal proved meaningless since the strong correlation between the shape parameters a and b

TABLE 1
Best-Fit Parameters and the Corresponding Amplitude Ratios R of Para and Ortho Signals

Signal	t_{pr}	Model	T(K)	A_1	a_1(kHz^2)	A_2	a_2(kHz^2)	b_2(kHz)	R	$\Delta R/R$
FID		$f_g + f_{gs}$	4.2	5.40 ± 0.06	117 ± 2	25.98 ± 0.02	0.920 ± 0.003	3.317 ± 0.002	0.208	0.012
FID		$f_g + f_{gj}$	4.2	5.40 ± 0.06	107 ± 2	25.84 ± 0.02	0.645 ± 0.003	4.058 ± 0.002	0.209	0.012
FID		$f_{gs} + f_{gs}$	4.2	5.18 ± 0.08	64 ± 7	26.02 ± 0.02	0.924 ± 0.003	3.318 ± 0.002	0.199	0.016
FID		$f_g + f_{gs}$	2.0	7.60 ± 0.30	450 ± 20	56.20 ± 0.02	1.231 ± 0.003	3.600 ± 0.002	0.135	0.040
FID		$f_g + f_{gj}$	2.0	7.30 ± 0.30	400 ± 20	56.04 ± 0.03	0.925 ± 0.004	4.400 ± 0.003	0.130	0.042
FID		$f_{gs} + f_{gs}$	2.0	7.60 ± 0.50	450 ± 6500	56.20 ± 0.02	1.231 ± 0.003	3.600 ± 0.002	0.135	0.066
DQ	25	$f_g + f_{gs}$	4.2	4.30 ± 0.06	107 ± 3	20.80 ± 0.20	0.860 ± 0.030	3.220 ± 0.030	0.207	0.024
DQ	50	$f_g + f_{gs}$	4.2	3.82 ± 0.03	112 ± 2	17.87 ± 0.08	0.850 ± 0.020	3.270 ± 0.020	0.214	0.012
DQ	100	$f_g + f_{gs}$	4.2	3.78 ± 0.03	110 ± 3	16.69 ± 0.05	0.880 ± 0.020	3.350 ± 0.010	0.226	0.011
DQ	150	$f_g + f_{gs}$	4.2	3.55 ± 0.03	106 ± 2	15.65 ± 0.03	0.846 ± 0.008	3.408 ± 0.007	0.227	0.010
DQ	200	$f_g + f_{gs}$	4.2	3.34 ± 0.03	98 ± 2	14.93 ± 0.03	0.865 ± 0.007	3.462 ± 0.006	0.224	0.011
DQ	25	$f_g + f_{gs}$	2.0	8.35 ± 0.08	600 ± 10	41.00 ± 0.30	1.070 ± 0.040	3.590 ± 0.040	0.204	0.017
DQ	50	$f_g + f_{gs}$	2.0	7.96 ± 0.05	580 ± 10	40.10 ± 0.20	1.310 ± 0.020	3.480 ± 0.020	0.199	0.011
DQ	100	$f_g + f_{gs}$	2.0	7.65 ± 0.07	550 ± 10	37.17 ± 0.07	1.240 ± 0.020	3.620 ± 0.010	0.206	0.011
DQ	150	$f_g + f_{gs}$	2.0	7.22 ± 0.06	620 ± 10	34.33 ± 0.05	1.229 ± 0.009	3.672 ± 0.008	0.210	0.010
DQ	200	$f_g + f_{gs}$	2.0	7.11 ± 0.07	620 ± 10	33.10 ± 0.04	1.261 ± 0.009	3.754 ± 0.007	0.215	0.011

Note. The relative standard error of the amplitude ratio R is calculated from $|\Delta R/R| \leq |\Delta A_1/A_1| + |\Delta A_2/A_2|$.

deteriorates the stability of the fitting process, which is indicated by a huge increase in their standard errors (for a see a_1 in Table 1). The standard error of the parameter b_1 (not tabulated) increased even more abruptly with decreasing temperature.

The FID shapes of solid D_2 ($X \approx 0.33$) at temperatures of 2, 3, and 4.2 K were found to be well described by a sum of two analytical curves,

$$S_{\mathrm{FID}}(t) = \sum_{I=1}^{2} F_I(t), \qquad [12]$$

where $I = 1$ for the para and 2 for the ortho signal. The parameters A, a, and b of the fitting model are indexed correspondingly. The nearly perfect best fits of the model $f_g + f_{gs}$ are shown in Fig. 3. The best-fit parameters for alternative models are shown in Table 1. At 4.2 K the amplitude ratio R is in rather good agreement with the expected value $R = 0.2$ for all models listed. However, at 2 K the corresponding result clearly underestimates the amplitude of the para signal.

The substitution of Eq. [12] into Eq. [10] gives the fitting function for the DQ filtered signal,

$$S_{\mathrm{DQ}}(t_{\mathrm{pr}}, t) = \tfrac{1}{2} \sum_{I=1}^{2} [F_I(t_{\mathrm{pr}} - t) - F_I(t_{\mathrm{pr}} + t)]. \qquad [13]$$

Two analytical models were tested with Eq. [13]. In the model $f_{gs} + f_{gs}$ the shape parameters of the para signal proved again unstable but the combination $f_g + f_{gs}$, which was the best model with FIDs, worked well also with the DQ experiments. The best fits of Eq. [13], using the model $f_g + f_{gs}$, to the DQ filtered signals at 4.2 and 2 K are shown in Fig. 4. The middle curves in Figs. 4a and 4b are shown in the same arbitrary units as the curves in Figs. 1 and 3 but, in order to draw attention to the varying amplitude ratio of the narrow and broad maxima, the upper and lower curves are scaled so that all three curves have equal amplitudes for the broad maxima.

All of the fitting was performed with commercial software using the Levenberg–Marquardt algorithm. No weighting was used. The statistical results are summarized in Table 1. The standard errors are given as error limits of the parameters. The fitting functions are normalized so that each constant multiplier A_I equals the initial amplitude of the corresponding FID component. The best fit of Eq. [12] or [13] to the corresponding experimental data then gives the ratio of para and ortho concentrations in the sample as $R = A_1/A_2$.

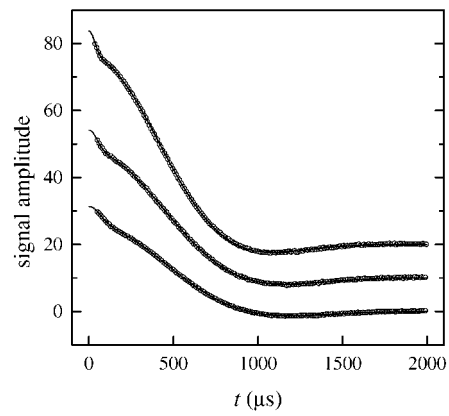

FIG. 3. Best fits of the model $f_g + f_{gs}$ to the FIDs at temperatures 4.2, 3, and 2 K from bottom to top, respectively.

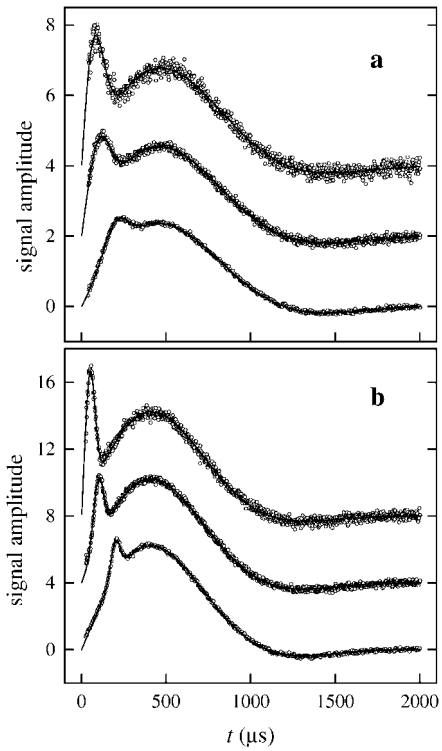

FIG. 4. Best fits of Eq. [10] using the model $f_g + f_{gs}$ to the DQ filtered signals at 4.2 K (a) and 2 K (b). The preparation times t_{pr} are 200, 100, and 50 μs from bottom to top. The middle curves in (a) and (b) have the same scaling as in Figs. 1 and 3 but the other curves are scaled so that the broad maxima have equal amplitudes.

In principle, both the FID and the DQ methods should give equal initial amplitudes. However, the DQ method yields somewhat lower absolute values for A_1, except for A_1 at 2 K, where the FID method fails. In the DQ experiment both A_1 and A_2 decrease with increasing preparation time t_{pr}. Also the amplitude ratio R varies but the relative changes are smaller and more random in nature.

4. CONCLUSIONS

We have shown that the pulse sequence 90°_ϕ–t_{pr}–90°_ϕ–t_{ev}–90°_x–t, consisting of three strong RF pulses ($\omega_1/2\pi \sim 80$ kHz), can be used to excite and detect DQ coherence in solid D_2. The detected signal is well interpreted in terms of the FID shape functions, evaluated at shifted times $t_{pr} \pm t$ (Eq. [13]). The corresponding amplitudes offer a promising method for determining the ratio of the para and ortho NMR signal amplitudes and thus also the para concentration (cf. the last two columns in Table 1). At 4.2 K the FID and DQ filtering methods can have a comparable success in the concentration determination, if the 90° RF pulse and the spectrometer dead time are short. However, at 2 K the DQ method is already clearly better. An examination of Figs. 3 and 4 indicates that in the case of the DQ experiment the statistical error of the fit can be diminished by increasing the number of averaged signals, which is not possible when using FIDs. Contrary to the FID method the DQ filtering seems to become more reliable with decreasing temperature, which provides an even more effective way to increase the signal-to-noise ratio.

Although the DQ filtered para signal becomes stronger and sharper with decreasing t_{pr} the lowest relative error of R is found when $t_{pr} \sim 150$ μs. This is probably due to the increased signal-to-noise ratio with increasing t_{pr}. However, the expected value of R is best reproduced by the signals measured with short preparation times. Experiments with longer t_{pr} tend to slightly overestimate the para concentration in the sample although many of them give the predicted result within the error limits.

The DQ filtering method can be used to determine the para concentration without any calibration, although the use of a sample with a known initial concentration may increase accuracy. In order to measure very low para concentrations, say less than 1% ($R < 0.004$), the standard error of the parameters A_1 and A_2 has to be lowered at least by one order of magnitude. This should be possible, when experiments are done at a lower temperature and more signals are averaged.

5. EXPERIMENTAL

The experimental setup was almost identical to that described in (*15*). The sample was prepared by a slow deposition of deuterium gas on the cold substrate at 4.2 K. During 30 min 2 mmol of D_2, originally at room temperature, was condensed on an area of about 95 mm^2. The thickness of the sample should be then about 0.5 mm.

The NMR detection was based on an old electromagnet which is used for X band ESR measurements and for proton NMR experiments at frequencies up to 30 MHz. However, with deuterons this means a resonance frequency of only 5.5 MHz. Hence, the resonance circuit of the old setup had to be modified. Because the NMR sensitivity of deuterons is only 100th of that of protons, special attention was paid to the sensitivity of the resonance circuit. The key words are high inductance and good filling factor of the NMR coil. Because our sample was a flat disc, both quantities could be optimized by making a short coil with many layers. Of course, in any coil the capacitive coupling between successive turns decreases the helical current during the pulse and also shunts part of the induced signal. In a multilayer coil, however, there is an additional coupling between successive layers which may be more critical because the voltage difference between neighboring turns, which belong to different layers, is higher than the voltage difference between successive turns.

In order to satisfy the condition $\omega_1 > \omega_Q$ required by the theoretical treatment we tried to make the 90° pulse as short as possible. The high power in combination with a relatively high inductance brought up an additional problem, namely sparking of the circuit. In a series resonance circuit a high inductance

results in a high quality factor $Q = \omega_0 L/R$, which in turn results in a high voltage over the reactive components. In an ideal circuit the maximum voltage over the capacitor as well as over the coil is Q times the amplitude of the pulse. That limits the usage of a multilayer coil where the first and last turns may be relatively close to each other. It is also worth noting that although the capacitance decreases with increasing inductance the physical size of the capacitor must be increased because of the sparking problems.

Our rough optimization procedure resulted in a monolayer coil with 60 turns followed by a cylindrical capacitor with about 3-mm-thick Teflon insulation between the cylinders. The coil was about the same size as in [(*15*), Fig. 1], 14 mm in diameter and 15 mm in length, but the capacitor was huge compared to that in the figure, about 10 mm in diameter and over 100 mm in length. Also the connection to the capacitor was different. The outer cylinder was grounded to the outer conductor of the NMR cable and the wiring from the coil to the inner cylinder of the capacitor was covered by about 1-mm-thick Teflon insulation. A 46-Ω resistor was used for impedance matching.

The Q value of that circuit was about 20 and the maximum pulse amplitude, which did not produce any sparking, was about 140 V. The sparking in such conditions is not surprising because $20 \cdot 140\ V = 2.8$ kV. However, it was a bit amazing that while testing the last version of the circuit in air we found that the electric discharge did not appear over the coil or through the insulation in the capacitor but just from the coil to open air.

In all of the experiments reported here only 90° pulses with a length of 3 μs were used and the number of averaged signals was 64 at 4.2 K and 32 at 3 and 2 K. The relatively long spin–lattice relaxation time $T_1 = 8.6$ s (measured at 4.2 K) limited the number of averaged signals. To be sure that the sample is relaxed when the pulse sequence starts we set the repetition time to 30 s, which was also kept constant during the whole series of experiments. Before fitting, all of the signals were normalized with respect to the number of averaged signals and the receiver gain of the spectrometer but the effect of the temperature on the amplitude was left as such.

In order to fulfill the conditions assumed in the theory the x component of the quadrature-detected signal was tuned carefully to zero. Unfortunately in the case of an electromagnet there is always some drift in the magnetic field appearing as a curvature in the x component. If it is possible to tune one of the quadratic components to zero the signal can be expressed as

$$y = f(t)\cos(\Delta\omega t + \phi) \quad \text{and} \quad x = f(t)\sin(\Delta\omega t + \phi),$$

where $f(t)$, $\Delta\omega$, and ϕ are the amplitude of the rotating magnetization, the offset in angular frequency units, and the deviation of the receiver phase from the y axis in the rotating frame, respectively. If the tuning is only slightly out of balance

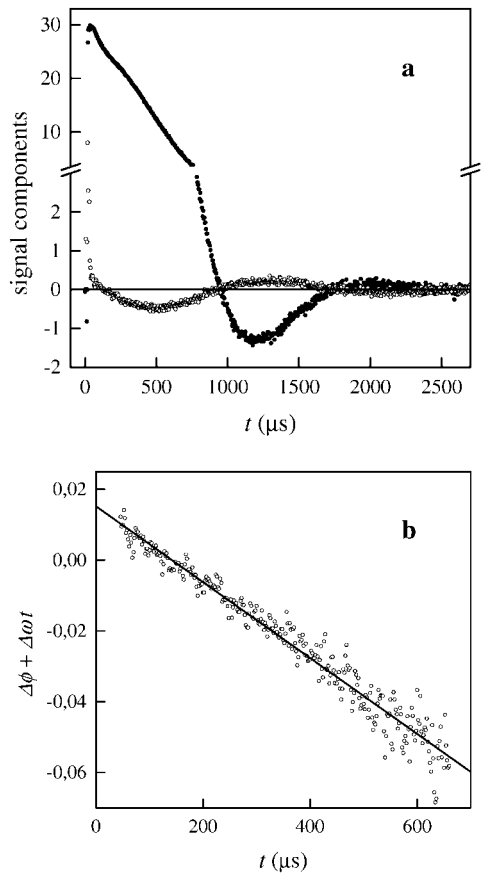

FIG. 5. The x (open circles) and y (solid circles) components of a slightly unbalanced FID (a) and the linear regression of $\Delta\omega t + \phi$ (straight line) to $\arctan(x/y)$ (open circles) in a selected range of the FID (b). The correlation coefficient of the fit, as high as 0.98, indicates that the absorption curve is symmetric and no information is lost when using this method for the phase correction.

we can assume that $f(t)$ is still the desired signal in the DQ experiment. The easiest way to extract $f(t)$ from the quadratic components is to make use of the formula $\sqrt{x^2 + y^2}$. Unfortunately this may result in an increased amplitude of the parts where the sign of the signal is determined by noise. In order to avoid this problem we used another method.

The phase angle $\Delta\omega t + \phi$ is equal to $\arctan(x/y)$, which gives a nice straight line for those parts of the signal where $y \gg x$ (Fig. 5). After computing the linear regression to that part we can extend $\Delta\omega t + \phi$ over the whole signal and extract $f(t)$ from the y component. Moreover, the linear behavior of $\arctan(x/y)$ proves that the x component does not contain any information, which is not tested when using the formula $f(t) = \sqrt{x^2 + y^2}$. In order to apply the $\arctan(x/y)$ method one has to keep in mind that the tuning must not deviate too far from the ideal, since the division of y by $\cos(\Delta\omega t + \phi)$ results in a large scatter of the corrected signal if the value of the argument starts to approach $\pm\pi/2$.

REFERENCES

1. W. N. Hardy and J. R. Gaines, *Phys. Rev. Lett.* **17,** 1278 (1966).
2. J. H. Constable and J. R. Gaines, *Phys. Rev. B* **3,** 1556 (1971).
3. D. Clarkson, X. Qin, and H. Meyer, *J. Low Temp. Phys.* **91,** 119 (1993).
4. X. Qin, D. Clarkson, and H. Meyer, *J. Low Temp. Phys.* **91,** 153 (1993).
5. A. B. Harris, H. Meyer, and X. Qin, *Phys. Rev.* **49,** 3844 (1994).
6. X. Qin and H. Meyer, *Phys. Rev.* **49,** 3857 (1994).
7. I. F. Silvera, *Rev. Mod. Phys.* **52,** 393 (1980).
8. A. Wokaun and R. R. Ernst, *J. Chem. Phys.* **67,** 1752 (1977).
9. S. Vega and A. Pines, *J. Chem. Phys.* **66,** 5624 (1977).
10. M. Punkkinen, A. Kaikkonen, E. E. Ylinen, M. Kankaanpää, and A. H. Vuorimäki, *Solid State NMR* **13,** 167 (1998).
11. A. Abragam, "The Principles of Nuclear Magnetism," Clarendon Press, Oxford (1961).
12. D. S. Metzger and J. R. Gaines, *Phys. Rev.* **147,** 644 (1966).
13. J. D. Sater and J. R. Gaines, *Phys. Rev. B* **37,** 1482 (1988).
14. V. Shevtsov, A. Scherbakov, P. Malmi, E. Ylinen, and M. Punkkinen, *J. Low Temp. Phys.* **104,** 211 (1996).
15. V. Shevtsov, P. Malmi, E. Ylinen, and M. Punkkinen, *J. Low Temp. Phys.* **114,** 431 (1999).